

# Microscopic simulation of symmetric boost fission with antisymmetrized molecular dynamics

Jingde Chen<sup>1,\*</sup>, Chikako Ishizuka<sup>2</sup>, Akira Ono<sup>3</sup>, and Satoshi Chiba<sup>2</sup>

<sup>1</sup>Nuclear Engineering Course, Transdisciplinary Science and Engineering, School of Environment and Society, Tokyo Institute of Technology, Tokyo 152-8550, Japan

<sup>2</sup>Laboratory for Zero-Carbon Energy, Institute of Innovative Research, Tokyo Institute of Technology, 2-12-1-N1-9, Ookayama, Meguro-ku, Tokyo 152-8550, Japan

<sup>3</sup>Department of Physics, Graduate School of Science, Tohoku University, 6-3, Aramaki Aza-Aoba, Aoba-ku, Sendai 980-8578, Japan

**Abstract.** We present our first results for a microscopic simulation of symmetric boost fission in terms of the antisymmetrized molecular dynamics (AMD) model. In AMD model, ground states of fissioning nuclei were prepared by a frictional cooling method and symmetrical boost momenta were given to nucleons inside to split the ground-state into fission fragments. After the simulation, we calculated the mass numbers and total kinetic energy (TKE) of the fission fragments. We also calculated orbital angular momenta of each fragment and identified them as spins, their mutual orientation and their orientation with respect to the linear momenta which defined the fission axis. Moreover, we found spin distribution of fission fragments was similar to the one given by the Fermi-gas model if spin cut-off parameter was adjusted. Finally, several ternary fission events were observed, emitting Tritium or <sup>4</sup>He from the neck region, and average energy and angles of these ternary particles with respect to the fission axis were found to be in accord with experimental data.

## 1 Introduction

Nuclear fission is identified as a complex large amplitude collective motion of quantum many-nucleon systems. However, even eighty years after its discovery [1], the microscopic mechanism of this phenomenon is yet to be fully understood. Also, there are many experiments on uranium and plutonium, but experimental nuclear data on MA (minor actinide) nuclides still remain insufficient. Since the nuclear data are indispensable for nuclear reactor [2] and nuclear transmutation technology [3], it is necessary to predict the unknown nuclear data by theoretical calculations. Therefore, we need a nuclear fission model that can understand the nuclear fission mechanism and predict the nuclear data.

Antisymmetrized molecular dynamics (AMD) model [4] is known to incorporate both the mean-field effects (as the TDDFT) as well as stochastic two-nucleon collisions similar to the cascade model. Due to these features, AMD model is capable of obtaining not only the “expectation value” or “mean trajectory”, but also “distributions” or “fluctuation” of observables.

In this research, we have simulated a symmetric fission of <sup>236</sup>U, <sup>240</sup>Pu and <sup>252</sup>Cf by a simple boost model by AMD. From the analysis of the results, we have obtained the total kinetic energy (TKE) of symmetric fission fragments and compared it with experimental data as verification of the AMD model. Moreover, we developed a new method for deriving spins of the fission fragments by

the AMD model, and calculated spins of fission fragments as the expectation value of the orbital angular momentum operator. By comparing the results with the values calculated by the time-dependent density functional theory and the spin distribution function from the Fermi-gas model, we verified the validity of the fission fragment spin distributions derived by the AMD model. Finally, we applied the AMD model to study the ternary fission in which tritium and  $\alpha$  particles were produced from the neck region. For nuclear data on the ternary fission, the third particle is emitted almost perpendicular to the fission axis and the kinetic energy values of ternary particles are measured [5]. We will verify whether the results of the method developed in this research can reproduce those experimental trends.

## 2 Method

In AMD model, the single nucleon wave function  $|\varphi_i\rangle$  is defined as below:

$$|\varphi_i\rangle = |\phi_i\rangle \otimes |\chi_i\rangle \otimes |\tau_i\rangle \quad (1)$$

$$\langle \mathbf{r} | \phi_i \rangle = \left( \frac{2\nu}{\pi} \right)^{3/4} \exp \left[ -\nu \left( \mathbf{r} - \frac{\mathbf{Z}_i}{\sqrt{\nu}} \right)^2 \right] \quad (2)$$

$$|\chi_i\rangle = |\uparrow\rangle \text{ or } |\downarrow\rangle \quad (3)$$

$$|\tau_i\rangle = |\text{Proton}\rangle \text{ or } |\text{Neutron}\rangle \quad (4)$$

The  $|\varphi_i\rangle$  is a direct product of the single particle wave function  $|\phi_i\rangle$ , the spin function  $|\chi_i\rangle$  and the isospin function  $|\tau_i\rangle$ .

\*e-mail: chen.j.ao@m.titech.ac.jp

The center of the Gaussian wavepacket is at  $\mathbf{Z}_i/\sqrt{v}$ , where  $\mathbf{Z}_i$  is a variational parameter.

In general, The variational parameter  $\mathbf{Z}$  has a real part  $\mathbf{D}$  and the imaginary part  $\mathbf{K}$  like Eqs(5).  $\mathbf{D}$  and  $\mathbf{K}$  are representing the expectation value of the position and the momentum.

$$\mathbf{Z} = \sqrt{v}\mathbf{D} + \frac{i}{2\hbar\sqrt{v}}\mathbf{K} \quad (5)$$

$$\mathbf{D} = \frac{\langle \phi_Z | \hat{r} | \phi_Z \rangle}{\langle \phi_Z | \phi_Z \rangle}, \mathbf{K} = \frac{\langle \phi_Z | \hat{p} | \phi_Z \rangle}{\langle \phi_Z | \phi_Z \rangle} \quad (6)$$

The total wave function for the A-body system is described by a Slater determinant as follows:

$$|\Phi(r_1, r_2, \dots, r_A)\rangle = \frac{1}{\sqrt{A!}} \det[\varphi_i(r_j)]. \quad (7)$$

Equation of motion of the total wave function is given by the following equation which stems from the time-dependent variational principle similar to the TDHF equation:

$$i\hbar \sum_{i\sigma} C_{j\tau, i\sigma} \dot{Z}_{i\sigma}^* = -\frac{\partial \langle \hat{H} \rangle}{\partial Z_{j\tau}} \text{ and } c.c \quad (8)$$

$$\text{where } C_{j\tau, i\sigma} \equiv \frac{\partial^2 \log \langle \Phi | \Phi \rangle}{\partial Z_{j\tau} \partial Z_{i\sigma}^*} \quad (9)$$

The  $\langle \hat{H} \rangle$  is the expectation of the Hamiltonian. In calculating the Hamiltonian, the Skyrme effective interaction set

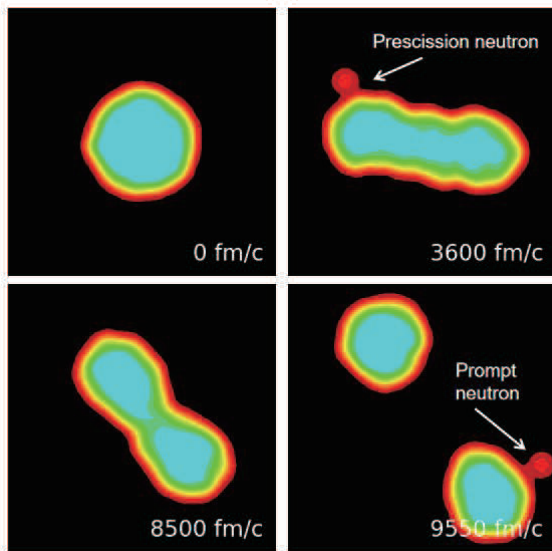


**Figure 1.** Snapshots of a  $^{236}\text{U}$  fission event which include emission of a pre-scission neutron and a prompt neutron simulated by AMD model

SLy4 [6] was used, neglecting the spin-orbit force. This parameter set was determined to reproduce the ground-state properties of neutron-rich nuclei and is appropriate for actinide nuclei.

In AMD fission simulations, as shown in Fig.1, the ground state of  $^{236}\text{U}$  calculated by the friction cooling method is an initial state and we gave the right-side and

left-side boost momentum as a trigger for the coherent collective motion. The boost momentum is about 53 MeV/c, giving an excitation energy of about 1.3 MeV per nucleon. The coherent collective motion is described by the equations of motion and two-nucleon collisions mentioned above. In this simulation, a pre-scission neutron is emitted at 3600 fm/c, and a prompt neutrons is generated from a fission fragment at 9500 fm/c, which shows that microscopic simulation such as realized by AMD is a sophisticated model to elucidate the fission phenomena.

### 3 Total Kinetic Energy of fragments, TKE

Fig.2 shows AMD calculated values of fission fragments' TKE in case of simulated fission of  $^{236}\text{U}$ . The color map in background is experimental data of  $^{236}\text{U}$  for incident thermal neutron, which shows two-peaks of fission plus a small components in between as the symmetric fission, which is the superlong mode in Brosa model. The white points are calculation results from the present AMD calculation for the symmetric boosted fission, and they gathered mostly at the center corresponding to the area of symmetric fission fragments.

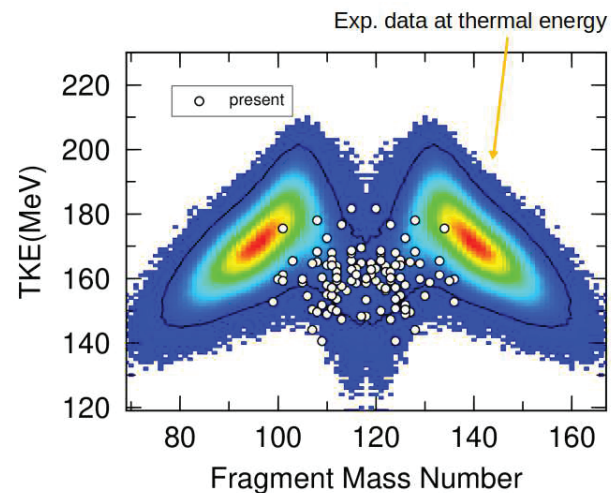


**Figure 2.** TKE of fission fragments of  $^{236}\text{U}$ . The white points denote results calculated by the AMD model, while the color scale show experimental information [7].

The present AMD calculation does not contain the shell effects due to absence of the spin-orbit force and due to the fact that the excitation energy is around 300 MeV. Therefore, the present calculation provides distributions clustered between 150 and 170 MeV and over about 10 units of mass number. The data are not separated according to symmetric and asymmetric fission modes. But, the population of symmetric fission products is much more than the asymmetric component, so the AMD model is focusing the symmetric fission.

## 4 Angular momentum

### 4.1 Average spin of fission fragments

Spins of the fission fragments are very important quantity in understanding fission, since the statistical decay of fragments are described by the Hauser-Feshbach theory, where conservation of angular momenta gives many constraint on the multiplicity and energy distributions of prompt neutrons and  $\gamma$ -rays, which affects distributions of the independent fission yields. Therefore, we discuss here how AMD yields spin distributions of fission fragments, how they are correlated to each other.

What we really calculate was the “rotational angular momenta”, which was defined as an expectation of the  $\mathbf{L} = \sum_j \mathbf{r}_j \times (-i\hbar \nabla_j)$ , where sum on  $j$  was taken over each of the fission fragment. Then, we identify absolute square of it to be equivalent to  $S(S + 1)$  of the corresponding fragment, and we call this “ $S$ ” as the fragment spin.

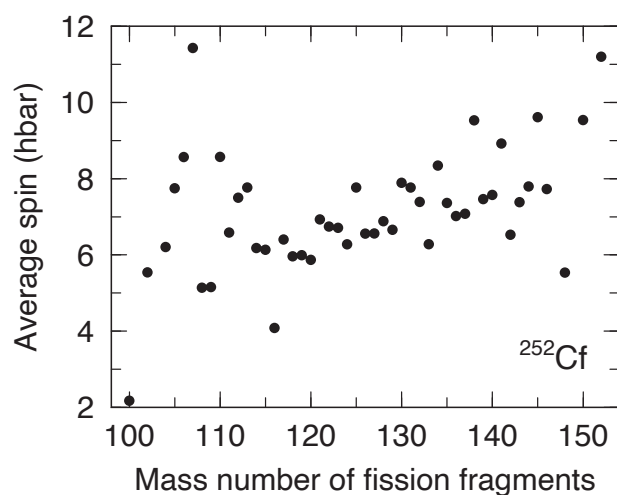


**Figure 3.** Spin distribution from  $^{252}\text{Cf}$  in AMD calculation and each point representing the average spin of each mass number of fission fragments

We present in Fig.3 the average spins of fission fragments as a function of the fragment mass number for fission of  $^{252}\text{Cf}$ . Even the AMD boost model is focusing the symmetric fission, there are still several asymmetric fission happened. As a result, light fragments and heavy fragment show a lot of scatter due to poor statistics. Wilson *et al* [8] has analysed the spins distribution of the asymmetric fission products which is a saw-tooth distribution. In contrast to their work, the AMD results show a more-likely linear increase of the average spin as the mass number of fission fragments in a symmetric component range.

This is a natural result since the shell effects are not present in the current calculation. Still, the absolute value of the spins range mostly from 4 to 12  $\hbar$ , and the whole average of spin for  $^{252}\text{Cf}$  is 6.8  $\hbar$  in AMD calculation.

### 4.2 Spin distribution

In the statistical model that deals with de-excitation of excited nuclei, the distribution function of spin  $S$  is given by

the level density formula of the phenomenological Fermi-gas model as follows.

$$\rho(S) \simeq \frac{(2S + 1)e^{-(S+0.5)^2/2\sigma^2}}{2\sigma^2} \quad (10)$$

where  $\sigma^2$  is referred to as the spin cut-off parameter. Therefore, it is an important question whether the microscopically calculated spin distribution function can be expressed by this functional form.

The green histograms in Fig.4 represent the spin distribution calculated by the AMD model. In the top Fig.4, triangles and squares are for fragments of  $^{236}\text{U}$  calculated with time-dependent density functional theory using SkM\* and SeaLL1 as DFT ingredients [9]. In the spin distribution, SkM\*-L and SeaLL1-L represent light fragment spins, and SkM\*-H and SeaLL1-H represent heavy fragment spins [10]. In this AMD calculation, symmetrical fission was simulated, so the result of this study is given as a green histogram as one distribution without distinguishing the light and heavy fission fragments. The black curve is the spin distribution function of the Fermi-gas model(4.2), with  $\sigma$  determined as  $2\sigma^2 = \langle S^2 \rangle$ , where  $\langle S^2 \rangle$  is the average squared spin calculated by AMD.

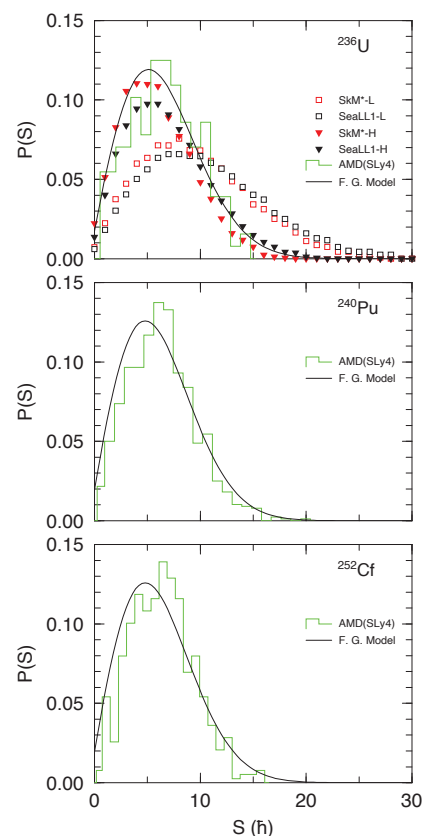


**Figure 4.** Spin distributions in cases of  $^{236}\text{U}$ ,  $^{240}\text{Pu}$  and  $^{252}\text{Cf}$

From the top of Fig.4 for  $^{236}\text{U}$ , we notice that the peak of the spin distribution of the heavy fission fragment by the time-dependent density functional theory is about  $5\hbar \sim 6\hbar$ , that of light fission fragment peak is at  $9\hbar$  to  $10\hbar$ . It is found that the AMD results are in good agreement with the heavy fragment results, and the Fermi-gas model can

reproduce them to a good approximation. In the results for  $^{240}\text{Pu}$  and  $^{252}\text{Cf}$  shown in the middle and bottom of Fig.3, both Fermi-gas model peaks are at  $5.3\hbar$ , while the AMD-calculated peak is slightly larger at Located near  $6\hbar$  to  $7\hbar$ , since AMD calculation is mainly reproduce the spin of symmetric fission fragments which are higher then the light fission fragments.

Fig.4 shows that the Fermi-gas model can nevertheless reproduce spin distributions calculated by the time-dependent density functional theory and AMD. It shows that the spin distribution given by the Fermi-gas model is a good approximation. It is surprising that these distributions, which are obtained based on different principles, agree with this accuracy, and it is an important reference for calculating the statistical decay of fission fragments.

## 5 Ternary fission

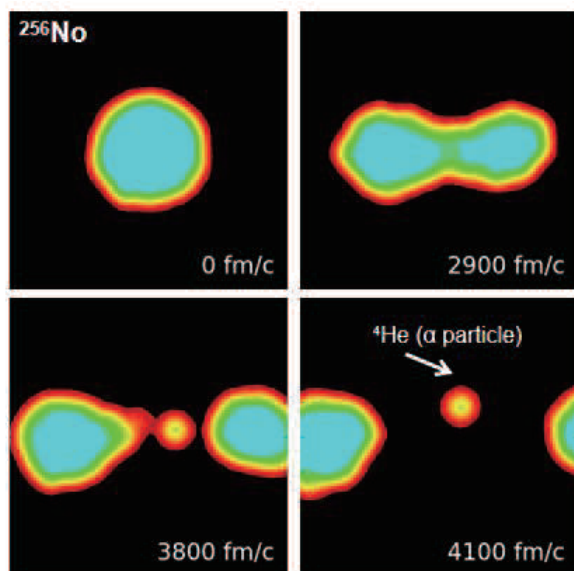


**Figure 5.** Snapshots of a fission event calculated by AMD which includes emission of a ternary particle

Ternary fission is a comparatively rare type of nuclear fission event in which three charged products are generated rather than two. The probabilities of ternary fission is approximately ranging from 0.2% to 0.4%. It is known that the third particles are produced from small nuclei as hydrogen ( $Z=1$ ) to nuclei such as argon ( $Z=18$ ). Although particles as large as argon nuclei may be produced as the third charged particle in the ternary fission, the most common third particle from ternary fission are  $\alpha$  particle, which make up about 90% of the third particle, and second-most common particle produced in ternary fission is  $^3\text{H}$  which makes up 7% of the ternary fission [11].

Experimentally, it is often interpreted that  $\alpha$  particles are found in fission products and that those  $\alpha$  particles are emitted within a shorter time than other evaporated neutrons from fission fragments and a longer range than other

$\alpha$  particles from  $\alpha$  decay. In other words, it is suggested that these  $\alpha$  particles are not produced by the evaporation of fission fragments, but are generated from the middle of fission fragments(neck region). Experimental data is also showing the fact that these third particles are ejected perpendicular to the fission axis owing to the ‘‘Coulomb focusing’’ mechanism. The results of the angular distribution of the ternary particle obtained by the AMD is in good accord with this mechanism.

## 6 Conclusion

We have developed the AMD model for simulating nuclear fission by giving a symmetrical boost momenta to the ground state of a fissioning nucleus. We found that the TKE and the expectation of the rotational angular momenta, which were identified as fragment spins, of the fission fragments are similar to other, more sophisticated theoretical calculation and experimental data. The spin distribution function of the phenomenological Fermi-gas model was found to fit well with AMD results. The model was also applied to the ternary fission, and the angular distribution of the emitted third particles was found to be concentrated in the direction perpendicular to the fission axis. Through these comparisons, it was found that the model developed based on the AMD model was an effective model that could give various information about the nuclear fission.

## References

- [1] O. Hahn, F. Strassmann, Über den Nachweis und das Verhalten der bei der Bestrahlung des Urans mittels Neutronen entstehenden Erdalkalimetalle, *Naturwissenschaften* **27**, 11 (1939).
- [2] D. Rochman, *et al.*, *Nucl. Data Sheets* **139**, 1 (2017).
- [3] G. Aliberti, G. Palmiotti, M. Salvatore, C. G. Stenberg, *Nuclear Science and Engineering*, **146:1**, 13-50 (2004).
- [4] Akira Ono, Hisashi Horiuchi, Toshiki Maruyama and Akira Ohnishi, *Progress of Theoretical Physics*, **87**, 5, 1185–1206 (1992).
- [5] G. M. Raisbeck, T. D. Thomas, *Phys. Rev.* **172**, 4 (1968).
- [6] E. Chabanat, P. Bonche, P. Haensel, J. Meyer, R. Schaeffer, *Nucl. Phys. A* **635**, 231 (1998).
- [7] M. D. Usang, F. A. Ivanyuk, C. Ishizuka, S. Chiba, *Sci. Rep.* **9**, 1 (2019).
- [8] J. N. Wilson, D. Thisse, M. Lebois, *et al.*, *Nature*, **590**, 566 (2021).
- [9] A. Bulgac, M. M. Forbes, S. Jin, R. N. Perez, N. Schunck, *Phys. Rev. C* **97**, 044313 (2018).
- [10] A. Bulgac, I. Abdurrahman, K. Godbey, I. Stetcu, *Phys. Rev. Lett.* **128**, 022501 (2022).
- [11] W. D. Loveland, A. W. Fairhall, I. Halpern, *Phys. Rev.* **163**, 1315 (1967).